

Paleostress evolution in the Canadian Cordilleran foreland fold-and-thrust belt west of Calgary

Veerle VANDEGINSTE^{1*}, Rudy SWENNEN¹, Jean-Luc FAURE², Kirk OSADETZ³ & François ROURE²

¹Department of Earth and Environmental Sciences, Section Geology, Katholieke Universiteit Leuven, Celestijnenlaan 200E, B-3001 Heverlee, Belgium

²Institut Français du Pétrole, 1&4 avenue de Bois-Préau, 92852 Rueil-Malmaison Cedex, France

³Geological Survey of Canada, 3303 – 33rd Street N.W., Calgary, Alberta

*Corresponding author: Veerle Vandeginste, Current address: Department of Earth Science and Engineering, South Kensington Campus, Imperial College London, London SW7 2AZ, United Kingdom (v.vandeginste@imperial.ac.uk)

ABSTRACT. A paleostress analysis was carried out on fault slip data collected at 13 sites distributed over a total of 135 km within the Canadian Rocky Mountains at a latitude of about N51°. Striae on brittle deformation structures were used to calculate paleostress states responsible for the observed deformation, and hence, to unravel the stress state evolution of the Cordilleran foreland fold-and-thrust belt in the study area. We identified five main paleostress states in the study area and interpret these as deformation events in the evolution of the foreland belt. Radial or pure (ENE-WSW) extension and oblique NE-SW to ENE-WSW compression were derived from back-tilted data and were probably active during an early stage. While radial extension may result from increasing burial in the absence of significant horizontal compression, the compression phase may correspond to Middle Jurassic to Late Cretaceous tectonic convergence along the western border of the North American craton. The other three paleostress states include (i) NE-SW to ENE-WSW compression, (ii) compressional NE-SW or pure strike-slip and (iii) pure or strike-slip extension or extensional strike-slip. The NE-SW to ENE-WSW compression and compressional or pure strike-slip phase correspond to the main tectonic compressive stress during Laramide orogeny, consistent with the stress field that caused the macrostructural thrust faults. The final extensional phase may relate to the Eocene regional extensional tectonics.

KEYWORDS: Canada, Cordillera, fault slip data, foreland fold-and-thrust belt, paleostress, stress inversion, tectonic evolution

1. Introduction

The Canadian Cordilleran geodynamic evolution is constrained mainly by large, commonly, map-scale deformation structures. In the foreland fold-and-thrust belt, abundant NW-SE trending thrust faults have been related to the primary NE-SW compression of the Laramide orogeny (Price, 1994). The analysis of minor brittle faults can be useful too, since meso-scale tectonic structures may identify and (relatively) date additional local and regional deformation phases that cannot be discerned from the analysis of the deformation structures. The latter relates to the fact that formation of primary or reactivation of pre-existing mesostructures may develop under moderate stress conditions that are too weak to deform older macrostructures (Eyal and Reches, 1983). In addition, mesostructural elements can display several sets of

crosscutting striae related to tectonic reactivation and thus provide the relative chronology of sequential stress fields (Sibson, 1990; Eyal et al., 2006). Homberg et al. (2002) analyzed minor faults to unravel pre-orogenic events in the thin-skinned fold-and-thrust belt of the French Jura Mountains showing that inherited faults influence subsequent deformation, impacting the fold-and-thrust belt development. Mesostructural analysis can be difficult in deformation belts, since these areas commonly record both pre- and post-orogenic extension which can complicate the reconstruction of paleostress evolution.

This study is a component of a combined structural and diagenetic-geochemical study of foreland fold-and-thrust belt faults and veins measured and sampled in the vicinity of the Trans-Canada Highway N°1. This combined project intends to provide insights into fluid flow evolution and its relationship to tectonics in the Canadian fold-and-

Site number and name	Longitude	Latitude	Age and formation	Thrust sheet	Location description
1 Moose Mountain South	114°50'W	50°48'N	Lower Carboniferous Rundle Group	Dyson Mountain	30 km SW of Bragg Creek, SW extension Highway N°66
2 Moose Mountain North	114°48'W	50°51'N	Lower Carboniferous Rundle Group	Prairie Mountain	5 km NW of site 1, along Highway N°66
3 McConnell	115°07'W	51°04'N	Cambrian Eldon Fm	McConnell	3.5 km E of Exshaw, along Trans-Canada Highway N°1
4 Lafarge Quarry	115°10'W	51°03'N	Upper Devonian Palliser Fm	Exshaw	Near Exshaw village, along Bow Valley Parkway 1A
5 Lower Exshaw	115°11'W	51°04'N	Mississippian Exshaw and Banff Fm	Exshaw	1.5 km NW of Exshaw along Bow Valley Parkway 1A
6 Upper Exshaw	115°14'W	51°03'N	Mississippian Exshaw and Banff Fm	Lac des Arcs	5.5 km NW of Exshaw along Bow Valley Parkway 1A
7 Upper Spray Lake	115°25'W	51°03'N	Devonian Palliser and Mississippian Exshaw and Banff Fm	Rundle	5 km SW of Canmore along road to Grassi Lakes
8 Banff	115°35'W	51°11'N	Mississippian Livingstone Fm	Rundle	1 km N of Banff along Trans-Canada Highway N°1
9 Rundle	115°34'W	51°11'N	Permian-Pennsylvanian Rocky Mountain Group and Triassic Sulphur Mountain Fm	Rundle	1.5 km W of Banff along Trans-Canada Highway N°1
10 Sulphur 1	115°37'W	51°10'N	Mississippian Exshaw and Banff Fm	Sulphur Mountain	3 km W of Banff along Trans-Canada Highway N°1
11 Sulphur 2	115°37'W	51°10'N	Mississippian Livingstone Fm	Sulphur Mountain	3.5 km W of Banff along Trans-Canada Highway N°1
12 Sunshine	115°41'W	51°08'N	Mississippian Livingstone Fm	Sawback	Along Sunshine Road, 1 km S of conjunction with Trans-Canada Highway N°1
13 Field	116°22'W	51°26'N	Cambrian Cathedral, Stephen and Eldon Fm	Sherbrooke Lake	9 km NE of Field village along Trans-Canada Highway N°1

Table 1. Geological information and location description of the sites studied

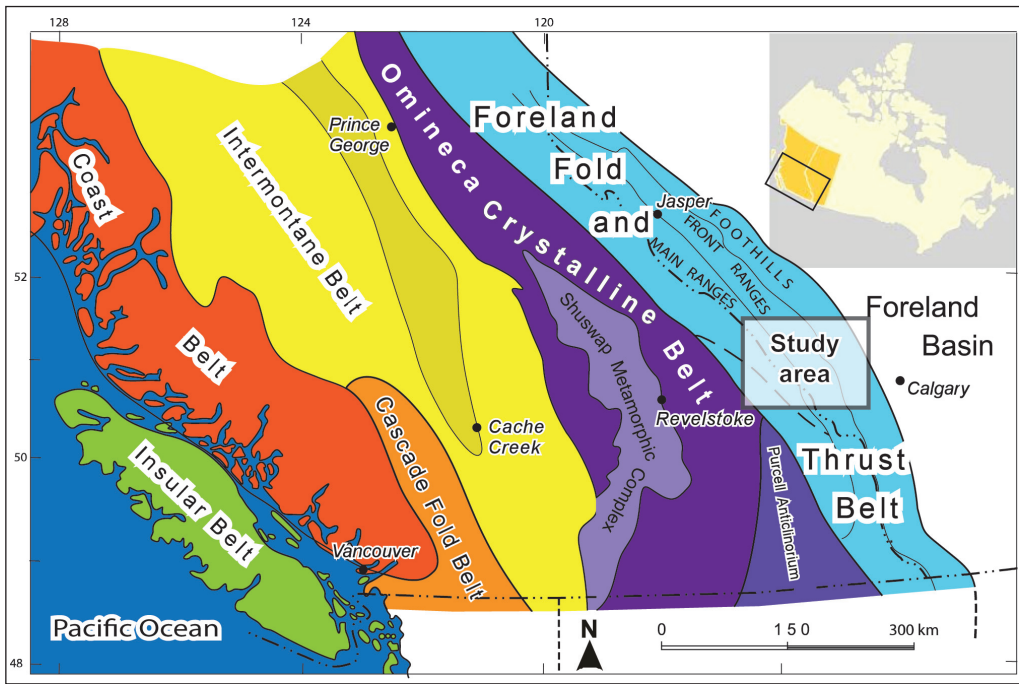


Figure 1. Southern Canadian Cordillera map with indication of tectonomorphological belts (modified from Gabrielse et al., 1991; Hardebol et al., 2009) and location of the study area west of Calgary. The study area, covering part of the Alberta – British Columbia border, is shown in detail in Fig. 2.

thrust belt study area. Recently, it has become more important to reconcile tectonics with fluid flow and diagenesis for multiple purposes. Recent age dating studies challenge existing models of Cordilleran evolution and the coupling among supracrustal deformation and geodynamic models of plate margin processes and terrane accretion events (e.g. Osadetz et al., 2004; van der Pluijm et al., 2006; Price, 2007). Major diagenetic processes, such as geographically pervasive, but time-transgressive synorogenic, but locally predeformational chemical remagnetizations remain unexplained (Enkin et al., 2000; Robion et al., 2004). Also the tectonic influences on petroleum systems, reservoirs and mineral resources in fold-and-thrust belts remain an active subject of research (e.g. Faure et al., 2004; Roure et al., 2005).

We report here the results and interpretations of a paleostress analysis, contributing to the knowledge on the evolution of paleostress

states in the Canadian Cordillera foreland fold-and-thrust belt. We carried out fault slip measurements on mesostructures at 13 sites (Table 1), distributed from the eastern Main Ranges (1 site), through the Front Ranges (10 sites), to the western Foothills (2 sites). The inferred paleostress states are compared to the paleostress analysis of the map-scale deformation structures and the stress history is inferred where meso-structures exhibit crosscutting relationships or superimposed striae.

2. Geological setting

The foreland fold-and-thrust belt is a northeastward tapering deformational belt that forms the eastern margin of the western Cordillera (including also the Omineca, Intermontane, Coast and Insular belts; Fig. 1) in Canada (Gabrielse and Yorath, 1991). The fold-and-thrust belt consists of deformed Mesoproterozoic to

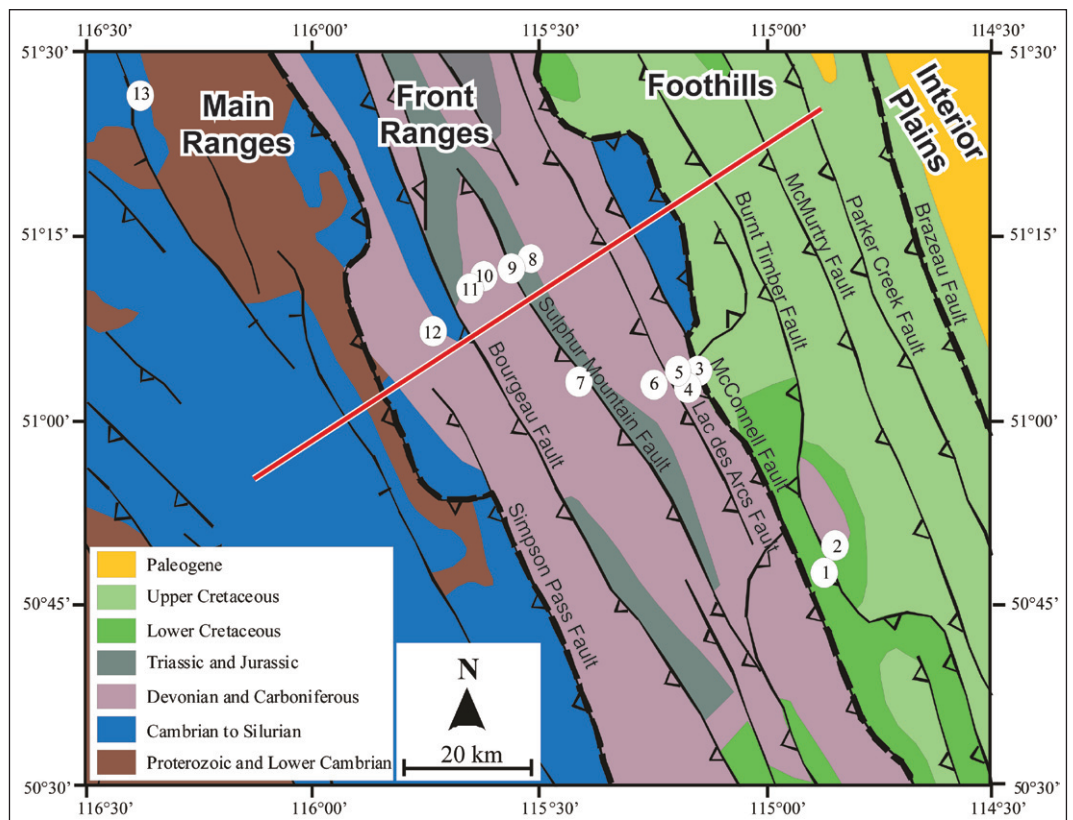


Figure 2. Simplified geological map (modified from Wheeler et al., 1996) showing the location of the sites studied. More information on the sites is presented in Table 1. Thick dashed lines indicate the borders between, from west to east, the Main Ranges, Front Ranges, Foothills and Interior Plains. The red line indicates the cross-section shown in Fig. 3. Fault names are shown on Fig. 3.

Paleogene successions from several depositional basins that were scraped off from the overriding North American craton and accreted to the overriding Intermontane terrane during Jurassic to Paleogene convergence between them (Monger and Price, 1979; Price, 1981; McMechan and Thompson, 1989; Price, 1994).

2.1. Proterozoic to Lower Jurassic evolution

The oldest deformed successions within the foreland belt are Mesoproterozoic and Neoproterozoic strata deposited in the Belt-Purcell and Windermere intracratonic rift basins during Proterozoic intracontinental rifting episodes within the Siberia-Laurentia-Australia “troika” (Sears and Price, 2003). The latter is a cratonic reconstruction that correlates Paleoproterozoic to Early Cambrian geological features among these three cratons, including their (2.0–1.7 Ga) Paleoproterozoic amalgamation, Mesoproterozoic and Neoproterozoic rifting, and latest Proterozoic (about 575 Ma) break-up, ocean basin formation and Cambrian thermal subsidence (Bond and Kominz, 1984; Monger and Price, 2002; Sears and Price, 2003).

Subsequent to the formation of the paleo-Pacific margin, foreland belt Upper Proterozoic to Lower Jurassic strata were deposited as a thick passive margin succession derived from the North American craton (Price, 1994). The plate margin changed from passive to convergent during the Middle Devonian at about 390 Ma (Monger and Price, 2002). Although there are few preserved Antler orogenic features in Canada (Root, 2001), the preserved pre-Late Devonian structures and wedge are inferred to be linked to the more extensively preserved Antler contractional structures and obduction in the southwestern United States Cordillera (Turner et al., 1989). Late Devonian and Carboniferous Kaskaskia subsidence both in the Cordilleran passive margin succession and on the cratonic platform (Price, 1994) is probably a “far-field” Antler orogenic effect, analogous to the Late Cretaceous–Paleogene Interior Seaway associated with the Cordilleran Orogeny (Feinstein et al., 1999).

2.2. Middle Jurassic to Paleocene evolution and main structures in the fold-and-thrust belt

Cordilleran-sourced foreland basin sedimentation started in the Middle Jurassic (Poulton, 1984; Asgar-Deen, 2003) and continued till the Paleogene. The Laramide Orogeny, expressed by Late Cretaceous to Paleocene oblique, dextral convergence between the Intermontane terrane and the North American craton resulted in thrusting in the southern Canadian Rocky Mountains (Engebretson et al., 1985; Price, 1994; Monger and Price, 2002). This developed the fold-and-thrust belt, which is commonly subdivided into four physiographic-tectonic zones, i.e. the Western Ranges, Main Ranges, Front Ranges and Foothills of the Rocky Mountains (Figs 1, 2). The eastern Main Ranges in the study area exposes the Lower Paleozoic basin-platform transition, differentiating cleavage development and folding in deep water shales and argillaceous limestones from thrusting in shallow water carbonate layers to the east. The Main Ranges are separated from the Front Ranges by the Simpson Pass thrust fault (Fig. 3). The Front Ranges are composed of steeply west-dipping thrust sheets of competent Paleozoic carbonates overlain by a thin Permo-Triassic succession, itself overlain by Jurassic and younger siliciclastics. The major Front Range thrust faults include the Bourgeau, Sulphur Mountain, Rundle, Inghismaldie, Lac des Arcs, Exshaw and McConnell

Mountain, Rundle, Inghismaldie, Lac des Arcs and Exshaw thrusts (Fig. 3). The eastern limit of the Front Ranges coincides with the McConnell thrust. In the footwall of the McConnell thrust, Middle Cambrian carbonates are thrust over a very large and prominent footwall “flat” in Upper Cretaceous clastic strata that extends south of the American border below the Lewis thrust. To the east are the Foothills, characterized by numerous steeply dipping imbricate thrust faults developed primarily in the Mesozoic and Tertiary siliciclastic succession.

The thrust faults described are mostly listric and northeasterly or easterly verging. The thrust faults commonly follow long bedding parallel detachments linked by ramps along which the faults change stratigraphic level more rapidly (Douglas, 1950; Bally et al., 1966; Dahlstrom, 1970; Price, 1981; Farmor, 1999). The thrusts merge downward into a basal detachment that converges with the contact with the underlying crystalline basement. The westward dipping basal detachment extends into the Cordilleran metamorphic core where it becomes ductile at mid-crustal levels (Price and Farmor, 1985).

2.3. Late Paleocene to recent evolution

By Late Paleocene to Middle Eocene, dextral transtension dominated in the south-central Canadian Cordillera (Ewing, 1980; Price, 1994) involving conspicuous east-west crustal extension and the tectonic exhumation of mid-crustal metamorphic rocks, including Archean and Paleoproterozoic basement rocks (Carr et al., 1987; Parrish et al., 1988; Constenius, 1996; Doughty and Price, 1999; 2000). This extensional stage was accompanied by westward increasing erosional exhumation of the foreland fold-and-thrust belt and the adjacent margin of the undeformed Interior Plains.

The contemporary stress regime in the Canadian Cordillera is dominated by NE-SW compression, where most focal mechanisms indicate strike-slip or thrust, except for a small zone in the Omineca belt, Quesnellia and the foreland belt where focal mechanisms indicate normal faulting (Bell et al., 1994; Mazotti and Hyndman, 2002; Ristau et al., 2007).

3. Paleostress inversion method

3.1. Basics

The principle behind the stress inversion method is the assumption that slip on a plane occurs parallel to the direction of the maximum resolved shear stress (Wallace, 1951; Bott, 1959). Hence, brittle structures that recorded slip movement (Fig. 4) can be used to reconstruct the corresponding stress state. By inverting collected fault-slip data (i.e. the fault plane orientation, the slip line orientation and the slip sense) the four parameters of the reduced stress tensor are determined, i.e. the principal stress directions σ_1 (maximum compressive stress), σ_2 (intermediate compressive stress) and σ_3 (minimum compressive stress) and the stress tensor shape factor or stress ratio $R = (\sigma_2 - \sigma_3) / (\sigma_1 - \sigma_3)$. The stress ratio R classifies the stress tensors as radial/pure/strike-slip extensive, extensive/pure/compressive strike-slip or strike-slip/pure/radial compressive stress states. Apart from Wallace (1951) and Bott’s (1959) assumption, applying the stress inversion method also assumes that the slip is independent, i.e. the fault

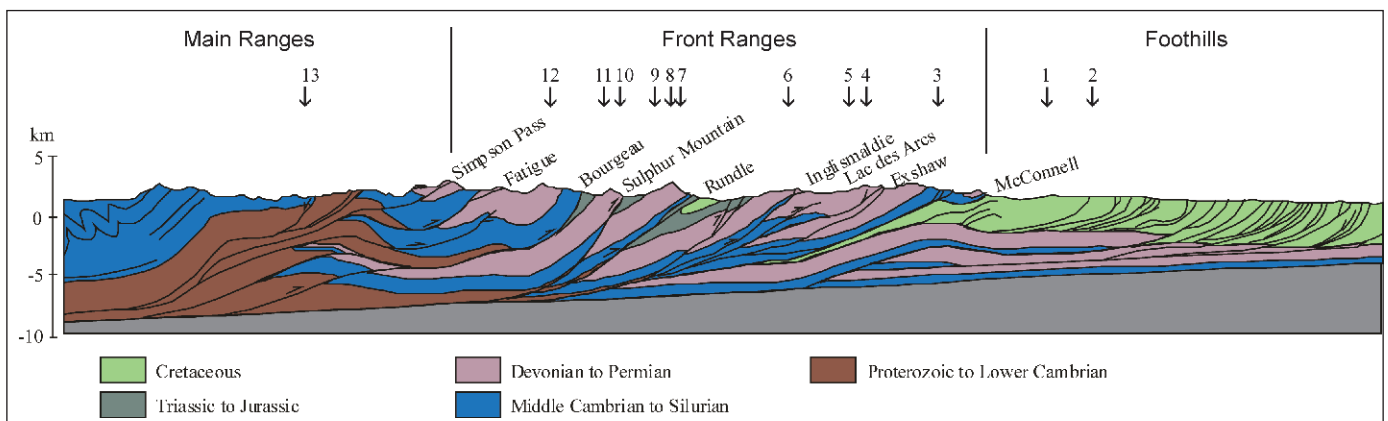


Figure 3. Cross-section (along the red line indicated in Fig. 2) showing the structure of the fold-and-thrust belt of the study area with indication of the main thrust faults and the sites studied (modified from Price and Farmor, 1985). The approximate location of the sites is projected on this cross-section.



Figure 4. Macrophotograph of striated normal fault plane at the Lower Exshaw (site 5).

movements should have no influence on the slip direction of other faults. In addition, one should be cautious in this method for slip sense misinterpretations and rotated rock fragments.

Several procedures have been proposed to calculate the best-fitting reduced stress tensor for a group of fault-slip data. The Direct Stress

Inversion method (Angelier, 1990) uses a least square algorithm to calculate the stress tensor, by minimizing the sum of the misfit angles, i.e. the angular difference between the measured slip vector and the calculated maximum shear stress vector, for all faults. The Numeric Dynamic Analysis or PBT method (Turner, 1953; Sperner et al., 1993) is based on the Mohr-Coulomb criterion, i.e. slip is only induced along a fault plane if friction is overcome by a high shear-to-normal stress ratio. The PBT method reconstructs a triple of mutually perpendicular kinematic axes that, assuming coaxial deformation, coincide with the stress axes. This involves the calculation of the orientation of the compression and tension axes (P and T axes respectively) for each fault (with B axis in the fault plane).

3.2. Stress inversion of heterogeneous data sets

Usually, not all brittle data belong to a single subset. This can be caused by the action of several tectonic events affecting the rocks. Hence, the raw data set needs to be separated into subsets to reconstruct paleostress evolution. In this respect, variations on the two methods mentioned were developed. For example, the Multiple Inverse method (Yamaji, 2000) separates paleostress states from a heterogeneous fault-slip data set that recorded changes in the stress state through time. This procedure uses the misfit angle, similar to the Direct Inverse method, and it calculates a reduced stress tensor for any possible subset of a number of faults. This method is a kind of cluster analysis, whereby each stress that activated a subset of faults correlates the members of the subset to each other. The Stress Inversion

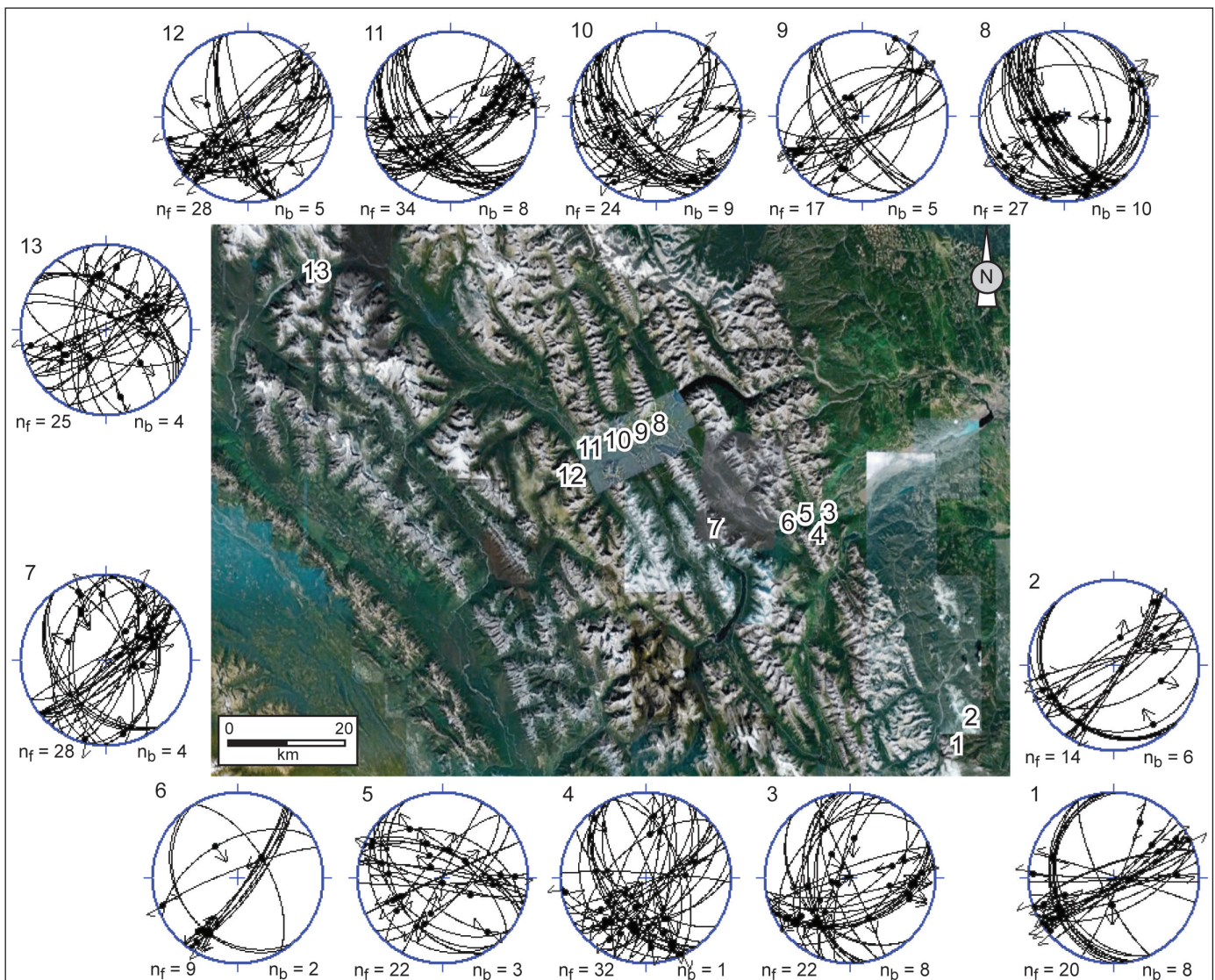


Figure 5. Google Earth image of the study area. Numbers indicated on the map refer to the different sites studied as listed in Table 1. Lower-hemisphere equal-area projection of bedding planes and striated fault planes (striated bedding planes have been excluded from the data set, as explained in the methodology) measured at each site. The amount of data presented in each stereogram is reported by n_f (number of striated fault planes) and n_b (number of bedding planes). The bedding has a general NNW-SSE to NW-SE orientation with dip towards the SW, except for site 13, in the Main Ranges, where it dips towards the NE.

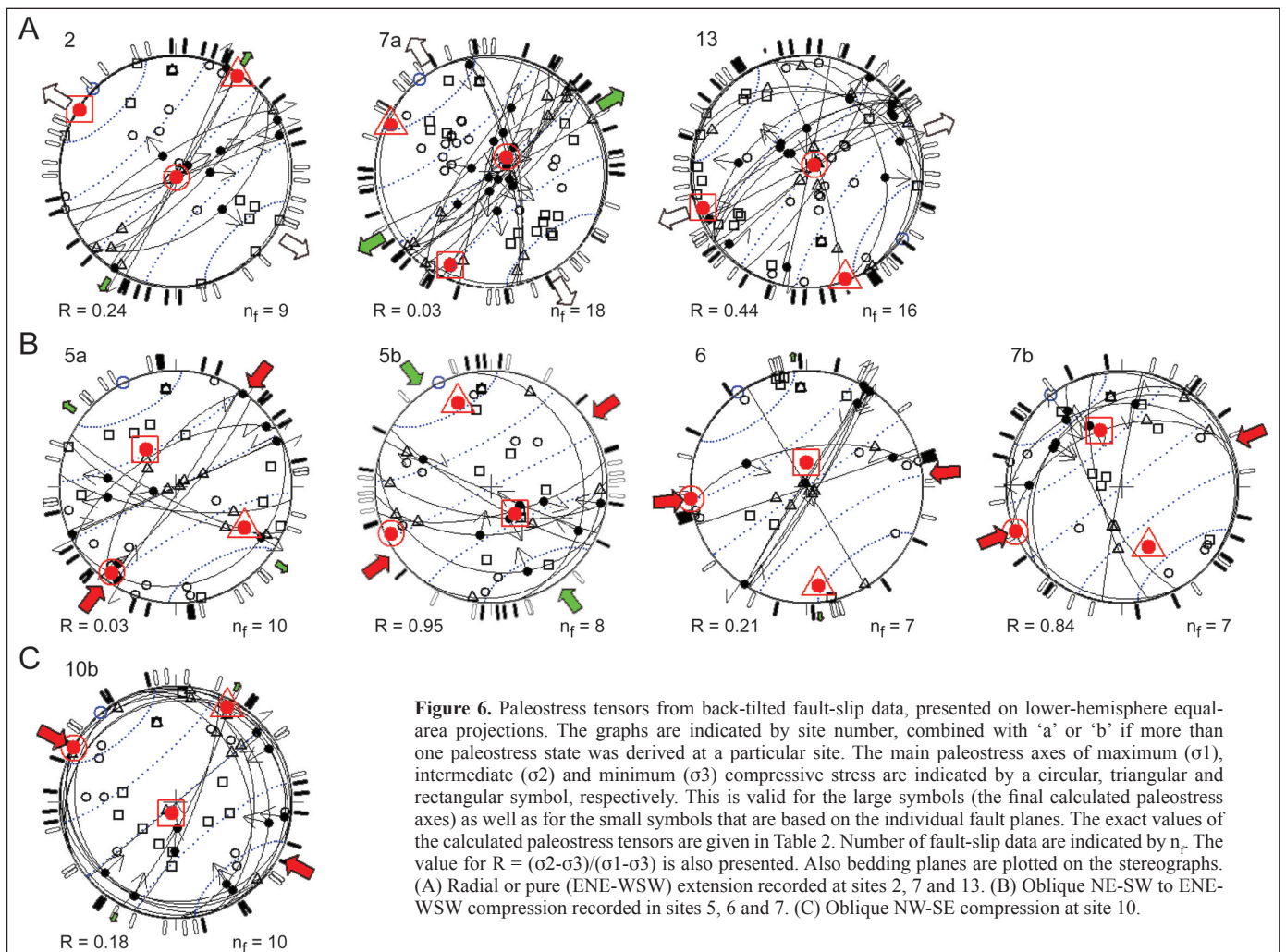
Site	n	nt	σ_1	σ_2	σ_3	R	ANG	Regime	
1	14	20	073/17	341/05	233/71	0.04	11	strike-slip compressional	post-tilt
2	9	14	175/86	033/03	303/02	0.24	4	radial extensional	pre-tilt
3	12	22	207/22	328/50	103/30	0.9	15	extensional strike-slip	post-tilt
3	7	22	247/04	025/84	157/03	0.32	18	pure strike-slip	post-tilt
4	20	32	215/22	078/61	313/17	0.28	9	compressional strike-slip	post-tilt
4	8	32	078/17	330/44	184/40	0.84	15	oblique compressive	post-tilt
5	10	22	217/09	121/32	321/56	0.03	5	oblique compressive	pre-tilt
5	8	22	245/06	338/24	139/65	0.95	19	oblique compressive	pre-tilt
6	7	9	264/00	173/16	359/73	0.21	5	oblique compressive	pre-tilt
7	18	28	047/75	295/06	203/14	0.03	8	radial extensional	pre-tilt
7	7	28	247/01	156/43	338/47	0.84	21	oblique compressive	pre-tilt
8	16	27	052/14	146/18	286/66	0.89	11	radial compressional	post-tilt
8	7	27	337/69	143/19	234/04	0.93	10	strike-slip extensional	post-tilt
9	12	17	218/04	101/78	308/09	0.09	4	compressional strike-slip	post-tilt
10	12	24	245/03	111/84	336/03	0.11	5	compressional strike-slip	post-tilt
10	10	24	298/01	028/08	200/82	0.18	13	oblique compressive	pre-tilt
11	21	34	186/81	008/08	278/00	0.72	10	pure extensional	post-tilt
11	9	34	055/14	319/22	175/63	0.26	14	pure compressional	post-tilt
12	18	28	249/59	069/30	339/00	0.64	6	pure extensional	post-tilt
13	16	25	049/83	160/03	251/07	0.44	8	pure extensional	pre-tilt

Table 2. Reduced paleostress tensors calculated from fault slip subsets. Orientation of the principal stress axes is given in direction/dip mode (expressed in degrees). n is the number of fault slip data per subset, nt is the total number of fault slip data per site, ANG is the average angle between the computed shear stress and observed striations (in degrees). Post-tilt or pre-tilt indicates whether the paleostress tensors were derived from the observed fault slip data or from bedding tilt corrected fault slip data, respectively.

Via Simulation method (Sippel et al., 2009) was also developed for the analysis of heterogeneous fault-slip data sets. It is a four-step procedure that combines the Multiple Inverse method (Yamaji, 2000) and the PBT-axes method (Turner, 1953; Sperner et al., 1993) with a final simulation of stress states.

3.3. Stress inversion approach in this study

For the paleostress analysis in our study, we used the computer program TENSOR developed by Delvaux and Sperner (2003) based on an improved version of the Right Dihedra Method (Angelier and



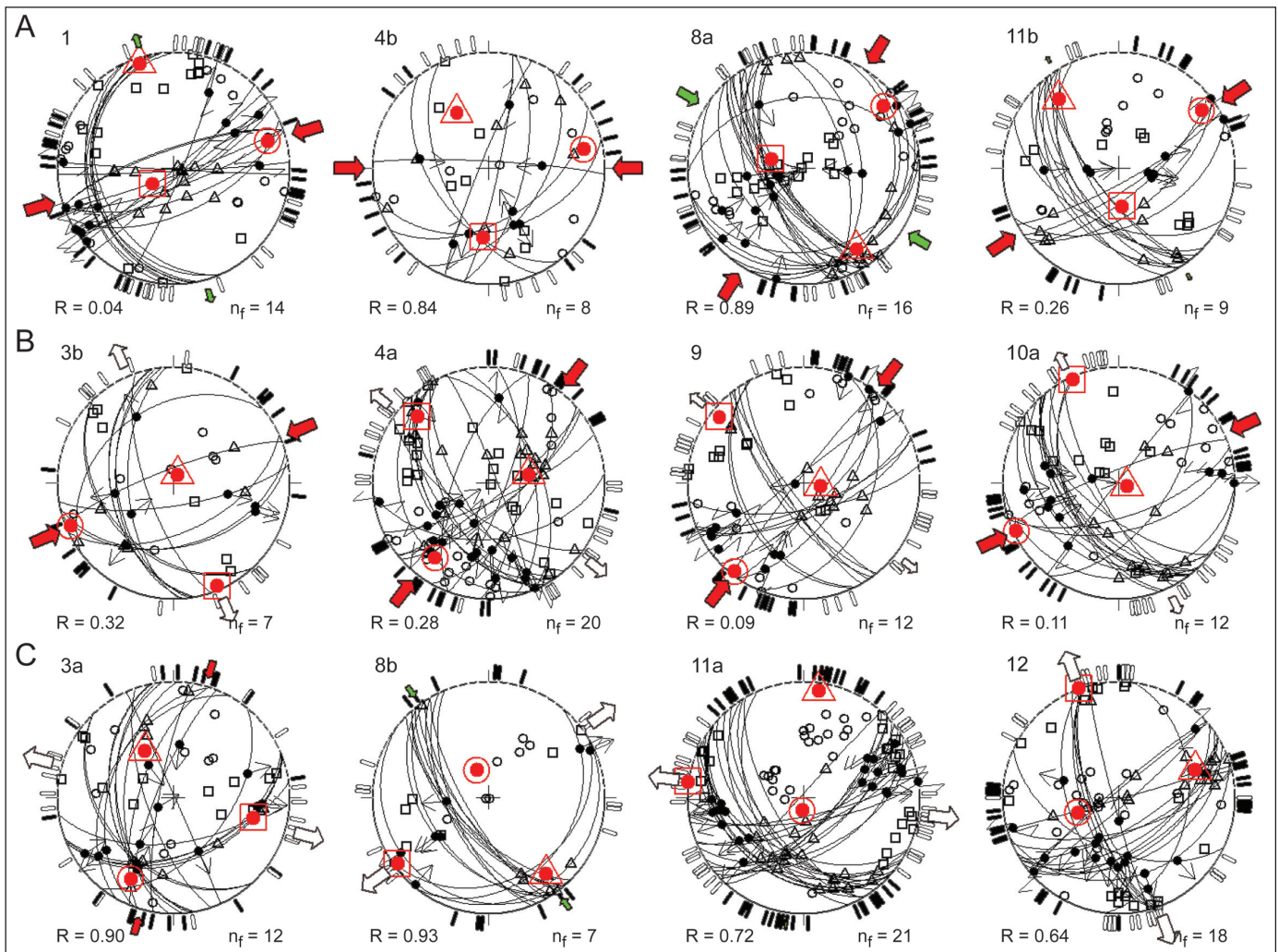


Figure 7. Paleostress tensors derived from fault-slip data, plotted on lower-hemisphere equal-area projections. Legend for symbols as in previous figure. (A) NE-SW to ENE-WSW compression recorded at sites 1, 4, 8 and 11. (B) Compressional NE-SW or pure strike slip at sites 3, 4, 9 and 10. (C) Pure or strike-slip extension or extensional strike-slip with variable extension direction at sites 3, 8, 11 and 12.

Mechler, 1977) in conjunction with a dynamic Rotational Optimization procedure. Separation of subsets from a heterogeneous data set is performed in an interactive and iterative way during stress inversion. Data separation into a subset and stress tensor optimization for that subset is carried out as a function of misfits determined with reference to the stress model calculated on the data set. The improved Right Dihedron method is characterized by: (i) estimate of the stress ratio R , (ii) applicability to both compression and tension fractures, and (iii) a compatibility test for data selection and separation. This method was typically designed for building initial data subsets from the raw data set, and for making a first estimation of the four parameters of the reduced stress tensor. This estimated stress tensor is subsequently used to initiate the search procedure of the Rotational Optimization method. The latter iterative inversion procedure was developed for interactive kinematic data separation of fault-slip data and progressive stress tensor optimization by testing different stress tensors to find the minimum value of the misfit function, as explained in Delvaux and Sperner (2003).

We performed the paleostress analysis on 302 fault slip data that we corrected for the magnetic declination. Although we also measured striated bedding planes in the field, our paleostress analysis does not include these striation data because they can be related to bed-on-bed slipping during folding based on the striae that are about perpendicular to the hinge line of the folds (Fig. 5). We collected these data at 13 sites in the study area in carbonate rocks of an age varying from Middle Cambrian to Permo-Triassic (Fig. 2); they are plotted together with non-striated bedding plane orientations in Fig. 5. A detailed location description and geological information of the outcrops, mainly located along the Trans-Canada Highway N°1, are summarized in Table 1. The slip sense indicators recorded in the study area are mostly calcite fibres (Fig. 4). The slip sense can be derived from accretion steps of slickenfibres, as they grow parallel to the movement direction of the

opposite block (congruous growth; Petit, 1987). We identified normal, reverse as well as strike-slip faults. Oblique-slip faults were attributed to the closest category, i.e. normal, reverse or strike-slip faults, based on the striae direction on the fault plane. For the subsets, separated in the paleostress analysis, for which the calculated two main paleostress tensors do not lie in the horizontal plane, but rather in the bedding plane, the paleostress analysis was redone on the bedding tilt corrected fault-slip data. This approach is based on the Andersonian model, whereby one principal stress is vertical and corresponds to the lithostatic pressure. By doing so, constraints on the relative timing were deduced, i.e. the paleostress tensors deduced from bedding tilt corrected values predate those deduced from the fault-slip data that were not corrected for bedding tilt.

4. Results

4.1. Paleostress states

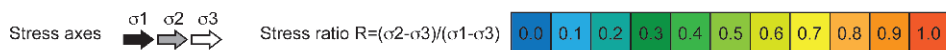
Our paleostress analysis of the collected fault slip data (raw data presented in Fig. 5) have resulted in a total of 20 reduced paleostress tensors, reported in Table 2. Most sites have a heterogeneous data set. Two different paleostress states were identified at 7 sites, whereas in other cases the number of outliers was not abundant enough to define a second subset and corresponding paleostress tensor. In total, we determined 9 compressional, 6 extensional and 5 strike-slip stress states. Eight of the 20 paleostress states were calculated from bedding tilt corrected fault slip data. These are presented in Fig. 6, while the paleostress states post-dating bedding tilt are presented in Fig. 7.

4.2. Constraints on the relative timing of paleostress states

The relative timing of paleostress states is usually constrained in two ways. First, the age of the rocks in which the fault occurs determines

Age	Site	Stress regimes					Constraints on relative chronology of subsets
		Pre-tilting		Post-tilting			
		Extension	Oblique compression	Compression	Strike-slip	Extension	
Permo-Triassic	9 Rundle						
Lower Carboniferous Rundle Group	1 Moose Mountain South						
	2 Moose Mountain North						
	8 Banff						post-tilt compression before extension subset
	11 Sulphur 2						
	12 Sunshine						post-tilt extension after bed-on-bed slipping
Lower Carboniferous Exshaw and Banff Fm	5 Lower Exshaw						pre-tilt compression before bed-on-bed slipping
	6 Upper Exshaw						
	10 Sulphur 1						
	7 Upper Spray Lake						
Devonian	4 Lafarge Quarry						
Cambrian	3 McConnell						post-tilt strike-slip before extension subset
	13 Field						

Figure 8. Synthesis of results, separated per rock age (and outcrop) and presented in chronological order, with indication of relative timing constraints. Stress ratio is colour coded.



the oldest possible age of the faulting event. Second, crosscutting relationships, such as intersecting and displaced faults or superimposed striae indicate the relative timing of the faulting events (e.g. Vandycke and Bergerat, 2001).

The age of the rocks studied varies from Cambrian to Permo-Triassic (Wheeler et al., 1996). The faulting events related to most of the derived paleostress states probably postdate the youngest (Permo-Triassic) rocks. This is especially true for the paleostress states that postdate bedding tilt, since the major tilting of the beds and related tectonic event is thought to have occurred during the Late Cretaceous - Paleocene Laramide Orogeny. The paleostress states that predate bedding tilt were determined in rocks of Cambrian to Lower Carboniferous age, which does not put strong constraints on the timing either (Fig. 8).

Some information on the relative chronology can be derived from crosscutting relationships (Fig. 8), although they are not abundant.

For example, at the McConnell outcrop (site 3) crosscutting faults determine the post-tilt strike-slip paleostress state to predate the extensional one. At the Banff outcrop (site 8), the post-tilt compression paleostress state is identified to predate the extensional state (striated planes with normal movement in Fig. 9A) based on intersecting striated faults. Striated bedding parallel planes are quite abundant (Fig. 9B) and can crosscut layer parallel shortening (or tectonic) stylolites (Fig. 9C). Faults intersecting with striated bedding parallel fault planes further indicate that the pre-tilt compressional paleostress state (at site 5) predates bedding parallel movement (resulting from bed-on-bed slipping, Roure et al., 2005), while the post-tilt extension state postdates this (at site 12). This is consistent with the previous mentioned constraints that identify the post-tilt extensional paleostress state as youngest phase and also with the Andersonian based determination of pre-tilt and post-tilt paleostress states.



Figure 9. Field photographs. (A) Striated normal fault planes at site 8. Hand as scale. (B) Bedding parallel striated planes at site 11. Hammer as scale. (C) Striated bedding parallel planes with reverse bed-on-bed slip and crosscutting the layer parallel shortening (or tectonic) stylolite at site 1. Hammer as scale.

5. Discussion

5.1. Cross-outcrop correlation of paleostress states

To derive stress states of regional importance (or stress fields), we first correlate the local paleostress states based on the direction of σ_1 . Only in a second step, we check the directions of the σ_2 and σ_3 axes and the stress ratio R , since they might represent local variations instead of differences between successive regional stress fields (Sippel et al., 2009). The relative timing of the stress states is either derived directly from field observations at the respective sites or indirectly from the findings at other sites. The total of 20 paleostress states derived from data collected in the different sites in the Western Canadian foreland belt study area can be classified in 2 pre-tilt (Fig. 6) and 3 post-tilt (Fig. 7) groups of correlated paleostress configurations. Hereby, we assume that the paleostress states that are similar in several outcrops and that are consistent with constraints on relative timing can be correlated and result from a paleostress state that has a more regional importance. The distinguished paleostress groups are:

(i) Radial or pure (ENE-WSW) extension is derived from bedding-tilt corrected fault slip data from sites 2, 7 and 13. This extensional state was detected in rocks of Cambrian to Lower Carboniferous age at sites in the Main Ranges, Front Ranges and Foothills. This state is characterized by a vertical σ_1 axis and relatively low stress ratio ($R \leq 0.4$). The orientation of the maximum extension axis varies between the different sites.

(ii) Oblique NE-SW to ENE-WSW compression paleostress states were calculated from bedding-tilt corrected fault slip data from sites 5, 6 and 7. A similar stress state was observed at site 10, with different direction of σ_1 (NW-SE) though. This pre-tilt compression state thus occurs in rocks of the Lower Carboniferous Exshaw and Banff Formations. At site 5, two subsets form part of this state; they are characterized by significantly different stress ratios with one paleostress state being compressional and the other rather strike-slip. All paleostress states of this group have a steep or subvertical σ_3 axis.

(iii) Post-tilt NE-SW to ENE-WSW compression is recorded at sites 1, 4, 8 and 11. The paleostress states are correlated by their similar σ_1 axis direction. The σ_3 axis is steep or subvertical and the stress ratio varies over a wide range ($R \leq 0.9$). The paleostress states of this group were derived from fault slip data in rocks of Devonian to Lower Carboniferous age.

(iv) Compressional NE-SW or pure strike slip was derived from fault-slip data collected at sites 3, 4, 9 and 10 in the Front Ranges. The

correlation of the local paleostress states is marked by the NE-SW direction of the σ_1 axis and the subvertical σ_2 axis. Also the stress ratio at the different sites is similar with $0.1 \leq R \leq 0.3$.

(v) The fifth state is a pure or strike-slip extension or extensional strike-slip with a range of extension directions. This state is derived from fault slip data collected at sites 3, 8, 11 and 12. Most of the local paleostress states have a subvertical σ_1 axis and are characterized by a high stress ratio ($0.6 \leq R \leq 0.9$).

5.2. Paleostress chronology

For the cross-outcrop correlation of the local paleostress states, we also assume that the different paleostress states occurred in the same chronology at each site and that the 5 paleostress states presented above are representative for the faulting events at least at the scale of the study area. An overview of the local paleostress states presented with rock age and ordered in chronological states is given in Fig. 8. As mentioned in the results section, the criterion of rock age does not put strong constraints on any of the paleostress states in our study. All of the states have a maximum age of Lower Carboniferous, except for the strike-slip state that has a maximum age of Permo-Triassic. A main chronology indicator used in our study is based on the Andersonian concept, which divides our results in states that were active before tilting of the layers and those active after tilting of the layers. Furthermore, crosscutting relations between faults and striated bedding parallel surfaces, related to bed-on-bed slipping during folding (Roure et al., 2005), confirm that the pre-tilt compression state predates the post-tilt extensional state. In addition to the arguments in Roure et al. (2005), Fig. 5 presents bedding parallel planes with striae that are about perpendicular to the hinge line of folds, and thus also consistent with the main compressive deformation responsible for the macrostructures, i.e. folds and later thrust faults in the foreland fold and thrust belt. Other crosscutting relationships observed in the field at sites 3 and 8 indicate that both post-tilt compression and strike-slip predate the extensional phase. Given these chronological indications, strong evidence is still lacking for the relative timing of pre-tilt extension and oblique compression and for the relative timing of post-tilt compression and strike-slip. However, we argue that pre-tilt extension predates oblique compression and that post-tilt compression predates strike-slip based on the following reasoning. For the relative chronology of the pre-tilt states, we argue that extension predates oblique compression based on the effect of 1) burial compression and 2) later tectonic compression. First, an extensional stress state with low stress ratio is expected to occur during burial due to a main vertical compressive stress and the lack of a strong horizontal compressive

stress at a relatively early stage in the geologic history of the rocks based on the tectonic history of the region (Price, 1994). This ENE-WSW extension cannot be related to extrados extension related to the folding process since in the latter case a different orientation would be expected based on the regional main tectonic events. Second, the pre-tilt oblique compressive state is then interpreted to reflect the initiation of the main NE-SW to ENE-WSW compression that subsequently caused folding and tilting of the rock layers. For our interpretation of the relative timing of post-tilt compression and later strike-slip state, we argue that both states are related to the Laramide orogeny (see discussion below) and that a transition of compression to strike-slip can be expected in an evolving thrust belt development with thrust faulting, i.e. change of a subvertical σ_3 axis to a subvertical σ_2 axis due to increasing burial weight by the thrust nappes (evidence of stacking of thrust nappes in Price, 1994).

As can be remarked in Fig. 8, there is a slight variation in the orientation of the stress axes in the different sites for individual stress states. This might indicate that individual thrust sheets had slightly rotated during thrusting. More likely, the slight variation is related to small differences in local stress due to the folded and faulted/fractured nature of the study area and the variation may also be caused by the relatively small data set that was limited to the amount of striated surfaces present in each outcrop.

5.3. Tectonic implications of our paleostress reconstruction and comparison with previous work in the Canadian Cordilleran foreland fold-and-thrust belt

Although the reconstruction of paleostress states using meso-structural brittle fault-slip data is widely and commonly applied, such studies are scarce in the Canadian foreland fold-and-thrust belt. This is, in part, because the mapping of deformation structures remains incomplete, but also because several early studies concluded that mesostructures (millimeter to meter-scale features) indicated only paleostress states that also caused the large deformation structures (e.g. Norris, 1958, 1964; Price, 1967; Castonguay and Price, 1995). For example, Price (1967), who proposed three different categories of "slickenlined fractures", including contraction, extension and transverse faults, concluded that these are kinematically consistent with the deformation structure. The author also observed other faults and inferred that these were pre-existing fractures reactivated during deformation or formed subsequent to flexural-slip folding and he considered these to be of minor significance. However, Eyal and Reches (1983) suggested that formation of primary and/or reactivation of pre-existing mesostructures may develop under moderate stress conditions insufficient to form new and/or reactivate older macro-structures, which highlights the importance of investigating mesostructures in addition to macrostructures. Feinstein et al. (1999) applied meso-structural analysis to the Moose Mountain culmination and did not employ the categorization proposed by Price (1967). They interpreted that all small-scale reverse faults in the study area formed during early deformation prior to tilting of the layers. They interpreted several phases in the deformation history and found that the earliest deformation was a shortening that was originally NE-SW to ENE-WSW that changed into an E-W shortening. In addition, they identified a younger, less intense NNE-SSW shortening.

Placing our paleostress results now in the regional tectonic context, we argue that the derived pre-tilt oblique compression, which postdates the Lower Carboniferous, was most likely active in Middle Jurassic to Late Cretaceous time due to convergent tectonic movements along the North American western border. Based on this, the timing of the pre-tilt extensional state can then be narrowed down to some time between Lower Carboniferous and Jurassic-Cretaceous. As mentioned above, pre-tilt NE-SW to ENE-WSW compression is also dominant in the mesostructures in the Moose Mountain area (Feinstein et al., 1999). The latter authors suggest that these mesostructures could have evolved simultaneously or at a late stage under the same general stress field that formed the macroscale thrust faults during the youngest deformation phase of the Rocky Mountain Front Ranges. However, we interpret that the pre-tilt compression phase precedes the macroscale thrust faulting, correlating the latter rather with the post-tilt compression and strike-slip.

The post-tilt compression and strike-slip states correspond to the Late Cretaceous to Paleocene transpression of the Laramide Orogeny (Price, 1994). The NE-SW to ENE-WSW compression direction is compatible with the orientation of the many macro-scale thrust faults

in the study area of the Rocky Mountains foreland fold-and-thrust belt. This direction has also been deduced in a study on paleostress derived from the anisotropy of magnetic susceptibility (Turner and Gough, 1983).

Finally, the derived post-tilt extension state, characterized by a wide range of σ_3 axis directions in our study probably developed during Eocene extension. Feinstein et al. (1999) report on a NNE-SSW shortening that postdates the NE-SW to ENE-WSW shortening and that could have developed or been reactivated after the general tilting. They suggest that this youngest shortening event represents an inboard effect of dextral strike-slip faulting along the Tintina Trench-Northern Rocky Mountain Trench fault zone transforming southwards into oblique convergence in the late Cretaceous to Paleocene time and southwestward into dextral slip during early and Middle Eocene via a large area of distributed shear and WNW-ESE crustal stretching (Price and Carmichael, 1986). Also in the United States Rocky Mountains, NNE-SSW shortening was documented and related to the opening of the Arctic Ocean during the middle Paleocene by Gries (1983). Thus, the period of compression and/or transpression ended relatively abruptly during early Eocene, when extension was linked, further north, to dextral N-S strike-slip faulting (Parrish et al., 1988). Evidence for Late Paleocene and Eocene dextral transtension is widely found in the Omineca and Intermontane Belts (Monger and Price, 2002). The beginning of extension is roughly coincident with changes in plate motion in the northeast Pacific, as outlined by Engebretson et al. (1985). Also Eyal et al. (2006) report faults trending N-S to NNE in the Okanagan portion of the Shuswap metamorphic core complex related to a regional Eocene E-W extension.

The fact that the fault planes show practically always only one striation direction argues that the interpreted paleostress states were derived from newly developed striated faults rather than from reactivated faults.

6. Conclusions

The paleostress study of brittle mesostructures carried out at 13 sites in the Canadian foreland fold-and-thrust belt, of which ten sites are situated in the Front Ranges, have revealed five main paleostress states, suggesting several deformation stages in the tectonic evolution of the foreland belt. Two paleostress states correspond to stages that predate tilting of the bedding and three paleostress states seem to postdate bedding tilt. We argue that pre-tilt radial or pure (ENE-WSW) extension and oblique NE-SW to ENE-WSW compression were active during an early stage. We interpret the radial extension was caused by increasing burial in the absence of significant horizontal compression, whereas the compression phase most likely corresponds to Middle Jurassic to Late Cretaceous tectonic convergence along the western border of the North American craton. The three post-tilt paleostress states consist of (i) NE-SW to ENE-WSW compression and (ii) compressional NE-SW or pure strike-slip, both corresponding to the main tectonic compression during the Laramide Orogeny consistent with the large thrust faults; and (iii) pure or strike-slip extension or extensional strike-slip, which can relate to the Eocene regional extensional phase.

7. Acknowledgements

This work was financially supported by the Research Fund of the Katholieke Universiteit Leuven (OT/01/27). The authors would like to thank the personnel of the Lafarge Company to grant access to their quarry. We appreciate and thank Parks Canada representatives for permission to sample in the National Parks. We thank the editor Jean-Clair Duchesne and both reviewers Sarah Vandycke and Manuel Sintubin for their constructive comments, which helped improving this manuscript.

8. References

- Angelier, J., 1990. Inversion of field data in fault tectonics to obtain the regional stress-III. A new rapid direct inversion method by analytical means. *Geophysics Journal International*, 103, 363-376.
- Angelier, J., Mechler, P., 1977. Sur une méthode graphique de recherche des contraintes principales également utilisable en tectonique et en séismologie: la méthode des dièdres droits. *Bulletin de la Société Géologique de France*, 7, 1309-1318.

- Asgar-Deen, M., Hall, R., Craig, J., Riediger, C., 2003. New biostratigraphic data from the Lower Jurassic Fernie Formation in the subsurface of west-central Alberta and their stratigraphic implications. *Canadian Journal of Earth Science*, 40, 45–63.
- Bally, A.W., Gordy, P.L., Stewart, G.A., 1966. Structure, seismic data and orogenic evolution of the southern Canadian Rockies. *Bulletin of Canadian Petroleum Geology*, 14, 337-381.
- Bell, J.S., Price, R.A., McLellan, P.J., 1994. Chapter 29: In-situ Stress in the Western Canada Sedimentary Basin. In: Mossop, G.D., Shetsen, I. (eds), *Geological atlas of the Western Canada Sedimentary Basin*. Canadian Society of Petroleum Geologists and Alberta Research Council.
- Bond, G.C., Komazin, M.A., 1984. Construction of tectonic subsidence curves for the early Paleozoic miogeocline, southern Canadian Rocky Mountains: Implications for subsidence mechanisms, age of breakup, and crustal thinning. *Geological Society of America Bulletin*, 95, 155-173.
- Bott, M.H.P., 1959. The mechanics of oblique slip faulting. *Geological Magazine*, 96, 109-117.
- Carr, S.D., Parrish, R.R., Brown, R.L., 1987. Eocene structural development of the Valhalla Complex, southeastern British Columbia. *Tectonics*, 6, 175-196.
- Castonguay, S., Price, R.A., 1995. Tectonic heredity and tectonic wedging along an oblique hanging wall ramp: the southern termination of the Misty thrust sheet, southern Canadian Rocky Mountains. *Geological Society of America Bulletin*, 107, 1304-1316.
- Constenius, K.N., 1996. Late Paleogene extensional collapse of the Cordilleran foreland fold and thrust belt. *Geological Society of America Bulletin*, 108, 20-39.
- Dahlstrom, C.D.A., 1970. Structural geology in the eastern of the Canadian Rocky Mountains. *Bulletin of Canadian Petroleum Geology*, 18, 332-406.
- Delvaux, D., Sperner, B., 2003. New aspects of tectonic stress inversion with reference to the TENSOR program. In: Nieuwland, D.A. (ed) *New insights into structural interpretation and modeling*. The Geological Society of London, Special Publications 212, 75-100.
- Doughty, P.T., Price, R.A., 1999. Tectonic evolution of the Priest River Complex, Northern Idaho and Washington: A reappraisal of the Newport fault with new insights on metamorphic core complex formation. *Tectonics*, 18(3), 375-393.
- Doughty, P.T., Price, R.A., 2000. Geology of the Purcell Trench rift valley and Sandpoint Conglomerate: Eocene an echelon normal faulting and synrift sedimentation along the eastern flank of the Priest River metamorphic complex, northern Idaho. *Geological Society of America Bulletin*, 112(9), 1356-1374.
- Douglas, R.J.W., 1950. Callum Creek, Langford Creek and Gap map-areas. *Geological Survey of Canada, Memoir*, 255.
- Engebretson, D.C., Cox, A., Gordon, R.G., 1985. Relative motions between oceanic and continental plates in the Pacific Basin. *Geological Society of America Special Paper*, 206, 59.
- Enkin, R.J., Osadetz, K.G., Baker, J., Kisilevsky, D., 2000. Orogenic remagnetizations in the Front Ranges and Inner Foothills of the Southern Canadian Cordillera: Chemical Harbinger and Thermal handmaidens of the deformation. *Geological Society of America Bulletin*, 112, 929-942.
- Ewing, T.E., 1980. Paleogene tectonic evolution of the Pacific Northwest. *Journal of Geology*, 88, 619-638.
- Eyal, Y., Osadetz, K.G., Feinstein, S., 2006. Evidence for reactivation of Eocene joints and pre-Eocene foliation planes in the Okanagan core-complex, British Columbia, Canada. *Journal of Structural Geology*, 28, 2109-2120.
- Eyal, Y., Reches, Z., 1983. Tectonic analysis of the Dead Sea Rift region since the Late Cretaceous based on meso-structures. *Tectonics*, 2, 167-185.
- Faure, J.-L., Osadetz, K., Benaouali, Z.N., Schneider, F., Roure, F., 2004. Kinematic and petroleum modeling of the Alberta foothills and adjacent foreland - west of Calgary. *Oil & Gas Science and Technology – Rev. IFP*, 59, 81-108.
- Feinstein, S., Eyal, Y., Bell, J.S., 1999. Implications of meso-structures for deformation history of the Moose Mountain structure, Canadian Rocky Mountain foothills. *Journal of Structural Geology*, 21, 55-66.
- Fermor, P., 1999. Aspects of the three-dimensional structure of the Alberta Foothills and Front Ranges. *Geological Society of America Bulletin*, 111, 317-346.
- Gabrielse, H., Yorath, C.J., 1991. Tectonic synthesis. In: Gabrielse, H., Yorath, C.J. (eds) *Geology of the Cordilleran Orogen in Canada*. Geological Survey of Canada
- Gries, R., 1983. North-south compression of Rocky Mountain foreland structures. In: Lowell, J.D., Gries, R. (eds) *Rocky Mountain Foreland Basins and Uplifts*. Rocky Mountain Association of Geologists, Denver, 9-32.
- Homberg, C., Bergerat, F., Philippe, Y., Lacombe, O., Angelier, J., 2002. Structural inheritance and cenozoic stress fields in the Jura fold-and-thrust belt (France). *Tectonophysics*, 357, 137-158.
- Mazzotti, S., Hyndman, R.D., 2002. Yakutat collision and strain transfer across the northern Canadian Cordillera. *Geology*, 30(6), 495-498.
- McMechan, M.E., Thompson, R.I., 1989. Structural Style and History of the Rocky Mountain Fold and Thrust Belt. In: Ricketts, B.D. (ed) *Western Canada Sedimentary Basin: A case history*. Canadian Society of Petroleum Geologists, 47-71.
- Monger, J.W.H., Price, R.A., 1979. Geodynamic evolution of the Canadian Cordillera – progress and problems. *Canadian Journal of Earth Sciences*, 16, 770-791.
- Monger, J., Price, R., 2002. The Canadian Cordillera: geology and tectonic evolution. *Canadian Society of Exploration Geophysicists Recorder*, 27, 17-36.
- Norris, D.K., 1958. Structural conditions in Canadian coal mines. *Geological Survey of Canada Bulletin*, 44: 54.
- Norris, D.K., 1964. Microtectonics of the Kootenay Formation near Fernie, British Columbia. *Bulletin of Canadian Petroleum Geology*, 12, 383-398.
- Osadetz, K.G., Kohn, B.P., Feinstein, S., Price, R.A., 2004. Foreland belt thermal history using apatite fission-track thermochronology: Implications for Lewis thrust and Flathead fault in the southern Canadian Cordilleran petroleum province. In: Swennen, R., Roure, F., Granath, J.W. (eds) *Deformation, fluid flow, and reservoir appraisal in foreland fold and thrust belts*, AAPG Hedberg Series, 1, 21-48.
- Parrish, R.R., Carr, S.D., Parkinson, D.L., 1988. Eocene extensional tectonics and geochronology of the southern Omineca Belt, British Columbia and Washington. *Tectonics*, 7, 181-212.
- Petit, J.P., 1987. Criteria for the sense of movement on fault surfaces in brittle rocks. *Journal of Structural Geology*, 9, 597-608.
- Poulton, T.P., 1984. The Jurassic of the Canadian Western Interior, from 49 degrees N latitude to Beaufort Sea. In Stott, D.F., Glass, D.J. (eds) *The Mesozoic of middle North America*. Canadian Society of Petroleum Geologists Memoir, 9, 15-41.
- Price, R.A., 1967. The tectonic significance of mesoscopic subfabrics in the southern Rocky Mountains of Alberta and British Columbia. *Canadian Journal of Earth Sciences*, 4, 39-70.
- Price, R.A., 1981. The Cordilleran foreland thrust and fold belt in the southern Canadian Rocky Mountains. In: McClay, K.R., Price, N.J. (eds.) *Thrust and Nappe Tectonics*. The Geological Society of London, Special Publication, 9, 427-448.
- Price, R., 1994. Cordilleran tectonics and the evolution of the Western Canada Sedimentary Basin. In: Mossop, G.D., Shetsen, J. (eds) *Geological atlas of the Western Canada Sedimentary Basin*. Calgary, Alberta: Canadian Society of Petroleum Geologists and Alberta Research Council
- Price, R.A., 2007. Fault dating in the Canadian Foreland: Evidence for late Cretaceous and early Eocene orogenic pulses: COMMENT. *GSA Journals Online Comment*
http://www.gsjournals.org/pdf/online_forum/i0091-7613-35-7-e134.pdf
- Price, R.A., Carmichael, D.M., 1986. Geometric test for Late Cretaceous-Paleogene intracontinental transform faulting in the Canadian Cordillera. *Geology*, 14, 468-471.
- Price, R.A., Fermor, P.R., 1985. Structure section of the Cordilleran foreland thrust and fold belt west of Calgary, Alberta. *Geological Survey of Canada, Paper*, 84-14.
- Ristau, J., Rogers, G.C., Cassidy, J.F., 2007. Stress in western Canada from regional moment tensor analysis. *Canadian Journal of Earth Sciences*, 44, 127-148.
- Robion, P., Faure, J.-L., Swennen, R., 2004. Late Cretaceous chemical remagnetization of the Paleozoic carbonates from the undeformed foreland of the Western Canadian Cordillera. In: Swennen, R., Roure, F., Granath, J. (eds) *Fluid flow, deformation history and reservoir appraisal in foreland fold and thrust belts*, AAPG Memoirs.
- Root, K.G., 2001. Devonian Antler fold and thrust belt and foreland basin development in the southern Canadian Cordillera: implications of the Western Canada Sedimentary Basin. *Bulletin of Canadian Petroleum Geology*, 49, 7-36.
- Roure, F., Swennen, R., Schneider, F., Faure, J.-L., Ferket, H., Guilhaumou, N., Osadetz, K., Robion, P., Vandeginste, V., 2005. Incidence and importance of tectonics and natural fluid migration on reservoir evolution in foreland fold-and-thrust belts. *Oil & Gas Science Technology – Rev. IFP*, 60, 67-106.
- Sears, J.W., Price, R.A., 2003. Tightening the Siberian connection to western Laurentia. *GSA Bulletin*, 115(8), 943-953.
- Sibson, R.H., 1990. Conditions for fault-valve behaviour. In: Knipe, R.J., Rutter, E.H. (eds) *Deformation Mechanisms, Rheology and Tectonics*. Geological Society Special Publication, 54, 15-28.
- Sippel, J., Scheck-Wenderoth, M., Reicherter, K., Mazur, S., 2009. Paleostress states at the south-western margin of the Central European Basin System – application of fault-slip analysis to unravel a polyphase deformation pattern. *Tectonophysics*, 470, 129-146.

- Sperner, B., Ratschbacher, L., Ott, R., 1993. Fault-striae analysis: a turbo pascal program package for graphical presentation and reduced stress tensor calculation. *Computers and Geosciences*, 19, 1361-1388.
- Turner, F.J., 1953. Nature and dynamic interpretation of deformation lamellae in calcite of three marbles. *American Journal of Sciences*, 251, 276-298.
- Turner, G.M., Gough, D.I., 1983. Magnetic fabric, strain and paleostress in the Canadian Rocky Mountains. *Tectonophysics*, 96, 311-330.
- Turner, R.J.W., Madrid, P.J., Miller, E.L., 1989. Roberts Mountain allochthon: Stratigraphic comparison with lower Paleozoic outer continental margin strata of the northern Canadian Cordillera. *Geology*, 17, 342-344.
- van der Pluijm, B.A., Vrolijk, P.J., Pevear, D.R., Hall, C.M., Solum, J., 2006. Fault dating in the Canadian Rocky Mountains: Evidence for late Cretaceous and early Eocene orogenic pulses. *Geology*, 34, 837-840.
- Vandycke, S., Bergerat, F., 2001. Brittle structures tectonic structures and palaeostress analysis in the Isle of Wight, Wessex Basin, Southern U.K. *Journal of Structural Geology*, 23, 393-406.
- Wallace, R.E., 1951. Geometry of shearing stress and relationships to faulting. *Journal of Geology*, 59, 111-130.
- Wheeler, J.O., Hoffman, P.F., Card, K.D., Davidson, A., Sanford, B.V., Okulitch, A.V., Roest, W.R., 1996. Geological Map of Canada. Geological Survey of Canada, 'A' Series Map 1860A.
- Yamaji, A., 2000. The multiple inverse method: a new technique to separate stresses from heterogeneous fault-slip data. *Journal of Structural Geology*, 22, 441-452.